

Citation for published version:

Isaac, P, Darby, A, Ibell, T, Evernden, M & Silva, P 2011, 'Plasticity based approach to analyse the response of FRP wrapped columns subjected to impact loads', Paper presented at Advanced Composites in Construction (ACIC 2011), Warwick, UK United Kingdom, 6/09/11 - 8/09/11 pp. 251-263.

Publication date:
2011

Document Version
Peer reviewed version

[Link to publication](#)

University of Bath

Alternative formats

If you require this document in an alternative format, please contact:
openaccess@bath.ac.uk

General rights

Copyright and moral rights for the publications made accessible in the public portal are retained by the authors and/or other copyright owners and it is a condition of accessing publications that users recognise and abide by the legal requirements associated with these rights.

Take down policy

If you believe that this document breaches copyright please contact us providing details, and we will remove access to the work immediately and investigate your claim.

Plasticity Based Approach for Evaluating the Blast Response of RC Columns Retrofitted with FRP

Philip Isaac, Antony Darby, Tim Ibell, Mark Evernden

Department of Architecture and Civil Engineering, University of Bath, Bath, BANES.

Corresponding author email: p.isaac@bath.ac.uk

[Received date; Accepted date. – to be inserted later]

Abstract

Work is presented on an incremental plasticity based analytical model to predict the peak displacement of FRP retrofitted RC columns subjected to blast loads. Tests have shown that columns retrofitted with transverse FRP display much higher levels of ductility and deform flexurally rather than failing in shear. This assumption is employed in the current model. In the proposed model the peak deflection is reached when the strain energy in the plastic hinges equals the supplied kinetic energy from the blast. Through the incremental approach the strain rates can be accurately and easily determined. The model is intended to assess the response of columns subjected to high energy blasts where large deflections would be expected and shows encouraging results when compared with experimental data. It also shows improved results compared with the more commonly used SDOF method.

1. INTRODUCTION

The increasing threat posed by terrorism has led engineers to investigate methods for strengthening and protecting our existing infrastructure. Research has demonstrated the potential for fibre reinforced polymers (FRPs) to strengthen a range of reinforced concrete (RC) members against blast loads, [1] and [2]. However, the application of this technology to blast situations is still limited due to a gap in fundamental understanding, suitable test data, informative design manuals and suitable analysis techniques.

The currently favoured analysis technique for the assessment of the structural response of RC members to blast loads is the equivalent single-degree-of-freedom (SDOF) method [3]. However, a number of issues have been raised over the method's ability to accurately represent the complicated response of a RC column to blast loading [4-6]. These issues include: determining dynamic reactions and shear resistance at high loading rates, selecting a suitable resistance function, determining strain rates accurately and incorporating them effectively in the analysis through material dynamic increase factors (DIFs) and accurately modelling the variation in the section stiffness as the column cracks during its deformation. Many believe that finite element (FE) methods provide a better alternative to the SDOF method. However, serious questions have been raised over the accuracy of these methods [7].

In response to some of these issues, particularly with respect to the accurate determination of strain rates, the current paper presents a novel incremental based plasticity model to predict the peak displacement of members deforming flexurally.

Typical failure modes for impulsively loaded RC columns are shown in Figure 1. These tests formed part of an experimental investigation using the state-of-the-art blast simulator at the University of California in San Diego (UCSD) [8]. Figure 1a shows how an un-retrofitted column, designed to US standards for non-seismic regions, failed catastrophically in shear whereas the same column design, retrofitted with Carbon FRP (CFRP) in the transverse direction (Figure 1b), showed a flexural deformation with plastic hinges forming at the supports and mid-height.

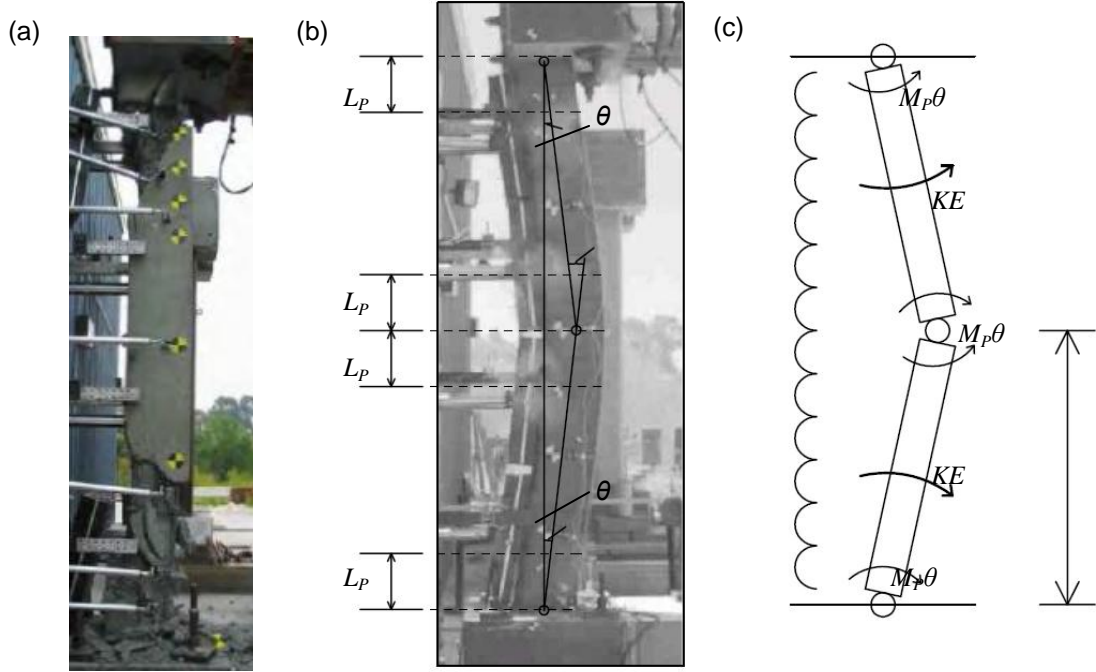


Figure 1. (a) Un-retrofitted column failed catastrophically in shear [8]. (b) Retrofitted column displaying flexural failure, with three plastic hinges drawn over (photo slightly obscured by dust) [4] (c) Idealised rigid body deformations of member

The primary advantage of the proposed model is the ease and accuracy with which strain rates can be determined and incorporated into the analysis. The discussion of this is the main focus of the current paper. Further to this the current model deals with an assumed mechanism for the real structure. This should make it easier in the future to extend the energy based approach to include other energy dissipation modes such as fragmentation of the concrete. The accuracy of the model has been best demonstrated on FRP wrapped RC columns responding in the impulsive range, as defined in Cormie *et al.* [9].

2. FORMULATION OF PLASTICITY MODEL

A flow diagram summarising the key stages in implementing the proposed plasticity model is shown in Figure 3. All calculations are carried out over small time steps and the total displacement and duration of response is found by summing the response from each time step. It is also important to note that the model assumes a rigid body mechanism, as shown in Figure 1c, from the beginning.

The proposed model requires the impulse from the blast to be converted into kinetic energy. When assuming rigid body rotations about fixed points, the derivation of this relationship differs from the case of linear motion as outlined below. Considering half the length of the column (between the end and central hinge positions, Figure 1c), the relationship between the rotational momentum and impulse is given by equation 1:

$$I_{half}\dot{\theta} = \int_0^t Q dt \quad (1)$$

where, $\dot{\theta}$ is the rotational velocity, Q is the moment about the end support caused by the force from the blast, given by equation 2,

$$Q = W(t) \cdot \frac{L}{2} \cdot \frac{L}{4} = \frac{W(t)L^2}{8} \quad (2)$$

where, $W(t)$ is the time dependent force per unit length from the blast (assuming the blast pressure is uniform along the column length) and L is the length of the column. I_{half} is the moment of inertia for half the column taken about the support, given by equation 3:

$$I_{half} = \frac{\frac{M_{tot}}{2} \left(\frac{L}{2}\right)^2}{3} = \frac{M_{tot} L^2}{24} \quad (3)$$

where, M_{tot} is the total mass of the column. Substituting equations 2 and 3 into equation 1 gives:

$$\frac{M_{tot} L^2}{24} \dot{\theta} = \int_0^t \frac{W(t) L^2}{8} dt \quad (4)$$

Equation 4 can be rearranged and written in terms of the impulse per unit length (i_e) as:

$$i_e = \int_0^t W(t) dt = \frac{M_{tot} \dot{\theta}}{3} \quad (5)$$

and the rotational kinetic energy for a half the column rotating about the support point is given by:

$$\frac{KE_{tot}}{2} = \frac{I_{half} \dot{\theta}^2}{2} = \frac{M_{tot} L^2 \dot{\theta}^2}{24 \times 2} \quad (6)$$

where, KE_{tot} is the total kinetic energy for the whole column. By squaring equation 5 and substituting into equation 6, for $\dot{\theta}$ can be eliminated. Since the impulse from the blast, i , is given by $i_e L$ (the impulse per unit length multiplied by the total length), the total kinetic energy acquired by the column from the blast impulse can be finally expressed as:

$$KE_{tot} = \frac{3i^2}{8M_{tot}} \quad (7)$$

It is assumed in the proposed model that the dissipation of the supplied energy is confined to the hinge regions. In order to determine the energy dissipated for a three hinge mechanism a small rotation (θ) is assumed from which the total energy dissipated, ED , can be determined through equation 8:

$$ED = M_p(\dot{\epsilon}) 4\theta \quad (8)$$

where $M_p(\dot{\epsilon})$ is the strain rate dependent plastic moment capacity of the section and 4θ is the sum of the rotations in the plastic hinges (Figure 1b).

The assumption for the hinge rotation is also important for determining the curvature in the hinge region which allows the moment capacity of the section to be found. As the calculation is performed over a small finite time step, the curvature in the section, which gives the strain profile, can also be used to obtain the strain rate profile in a very simplified, yet accurate manner. Once the strain and strain rate profiles are known a sectional method of analysis is used to determine the moment capacity of the member at any stage of the response. This method of analysis overcomes one of the significant issues raised with alternative analytical models in that they are not able to offer a simplified method for determining strain rates in the section.

A simplified method is finally presented to validate the assumed hinge rotation. This is achieved by comparing the displacement from the assumed hinge rotation with the displacement determined from the motion of the member during the time step.

This process is repeated for subsequent time steps until all of the energy supplied from the blast has been dissipated through plastic straining. The premise of this energy conservation approach is similar in principal to other methods of analysis, such as those used in the UFC manual [10].

The main benefits of the proposed model are the ease with which strain rates can be determined and directly incorporated in the analysis. Further to this the incremental approach makes it simpler to include the time varying nature of the applied load and more representative material characteristics such as strain hardening of the steel and concrete in tension. The following sections describe the precise formulation of the proposed model in more detail.

2.1 Plasticity theory and plastic hinges

Plasticity theory provides a simple yet accurate method for structural analysis by assuming that plastic deformations occur in specific regions where the moment in the section is highest. In a fixed-fixed condition (as might be expected with a column) plastic hinges develop in two phases as the load increases, firstly two hinges develop simultaneously at the supports, followed by a third hinge forming at the mid-span. The proposed model assumes that hinges form at the outset of the

4 Plasticity Based Approach for Evaluating the Blast Response of RC Columns Retrofitted with FRP

analysis. This allows the two halves of the column to be effectively treated as rigid bodies and the system as a whole can be treated as a mechanism. By assuming plastic hinges have formed, the member deforms as two rigid bodies (Figure 1c) and the rotations are confined to the plastic hinge regions. The curvature is assumed to be consistent over the whole hinge region. In the formulation of the proposed model, during each time step, a length for the plastic hinge (L_p) is assumed along with the rotation in the hinge (θ). From this it is possible to calculate the curvature (χ) in the section through eqn (9).

$$\chi = \theta / L_p \quad (9)$$

2.2 Layered sectional analysis

A layered sectional analysis of a reinforced concrete cross-section is an accurate method for determining the moment capacity of a member as shown by Wu *et al.* [11], for example. The technique divides the cross section into a number of layers of a finite thickness and the stress (σ), strain (ϵ) and in this case, strain rate ($\dot{\epsilon}$) are assumed to be uniform within each layer. It is assumed that plane sections remain plane and, therefore, the strain and strain rate profiles will vary linearly across the section. A schematic of the layered sectional analysis is shown in Figure 2.

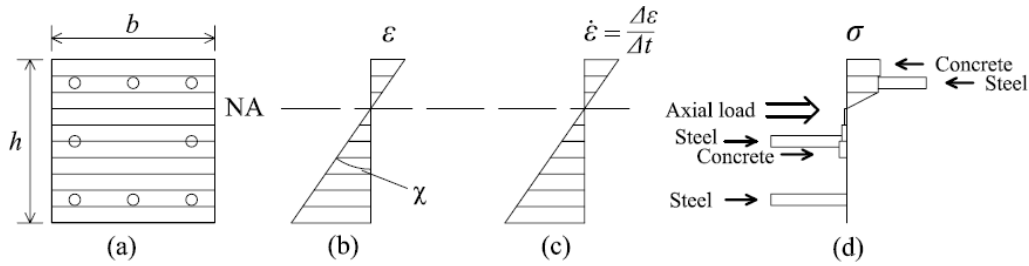


Figure 2. (a) Cross-section, (b) Strain profile, (c) Strain rate profile, (d) Stress block for a typical RC column member

Based on the curvature determined from equation 9 and shown in Figure 2b and by estimating the depth of the neutral axis (NA), the strain profile for a given hinge rotation (θ) can be established. The depth of the neutral axis is subsequently iterated to achieve equilibrium of forces in the section. The change in strain within each layer during the time step divided by the time step over which the calculation is being performed leads to the strain rate profile for the section, as indicated in Figure 2c. From these strain rates, the dynamic strength increase factors for the material in each layer can be calculated to provide the stress and, hence force in each layer.

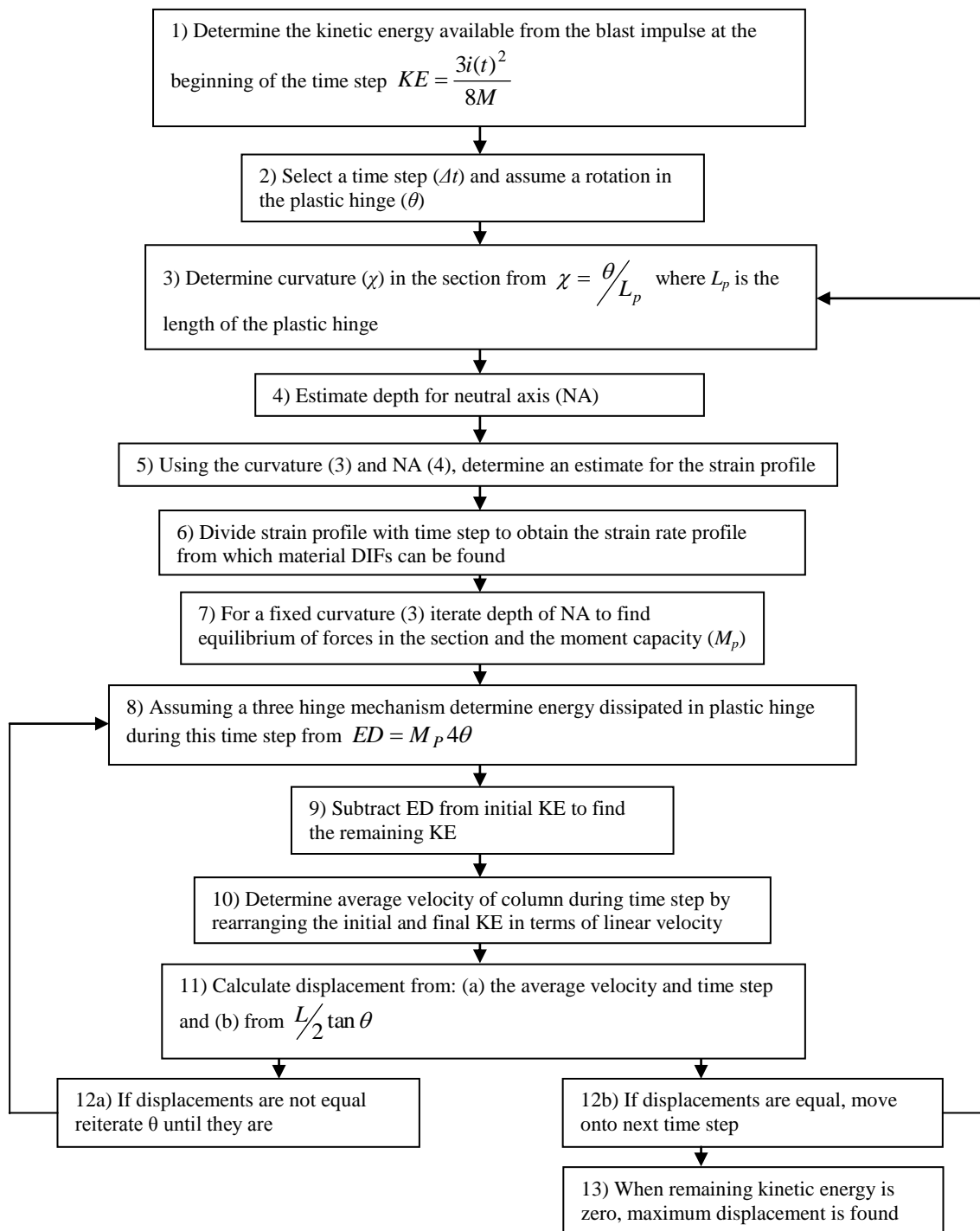


Figure 3. Flow diagram for implementing proposed model

2.3 Material dynamic increase factors (DIFs)

Both concrete and steel display strain rate dependent properties, although conflicting results have been reported for the exact stress-strain relationship of concrete at various rates of loading [12]. These characteristics are undoubtedly important when assessing the response of reinforced concrete members to high rate loading. Research has shown that at strain rates of 0.05 s^{-1} , as may be expected in earthquake situations, the moment capacity of a RC section could increase by 25% [13]. At higher rates of loading, as would be expected in blast situations, the increase would be even greater [5].

The dynamic increase factor is a convenient way to describe the change in the strength of the material as the strain rate varies. Specific relationships for concrete in compression and tension are shown in Figure 4a and b respectively and for reinforcing steel in Figure 5. The DIFs for concrete in tension are included due to the high increases in strength under high rate loading, up to a 700% increase in strength has been reported [14]. Concrete in tension is therefore included in the current model up to a limiting strain of

$$f_{ct}/E_c$$

where, f_{ct} is the ultimate tensile strength of the concrete (dependent on the strain rate) and E_c is the concrete's Young's modulus.

Standard DIF models have been adopted in the current formulation of the model. For concrete these are based on the bi-linear models determined by Malvar and Crawford [14] from the empirical data shown in Figure 4a and b. For the reinforcing steel, the relationship employed was based on the work of Malvar [15], shown in Figure 5.

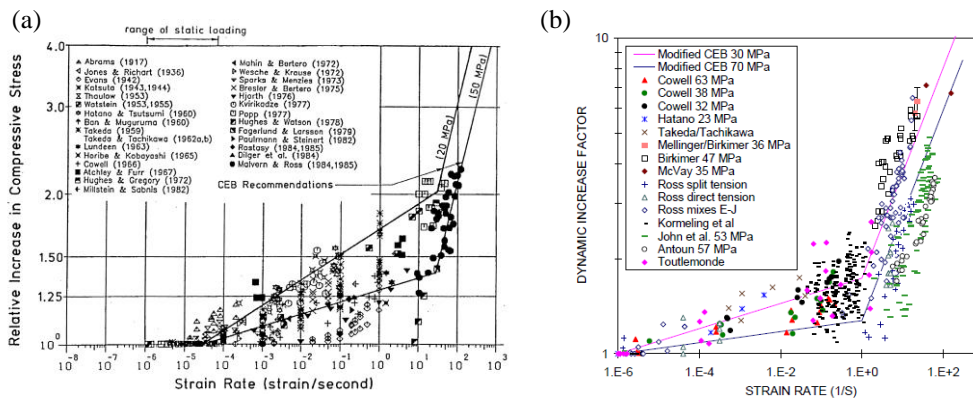


Figure 4. DIF for concrete: (a) in Compression [16] and (b) in Tension [14]

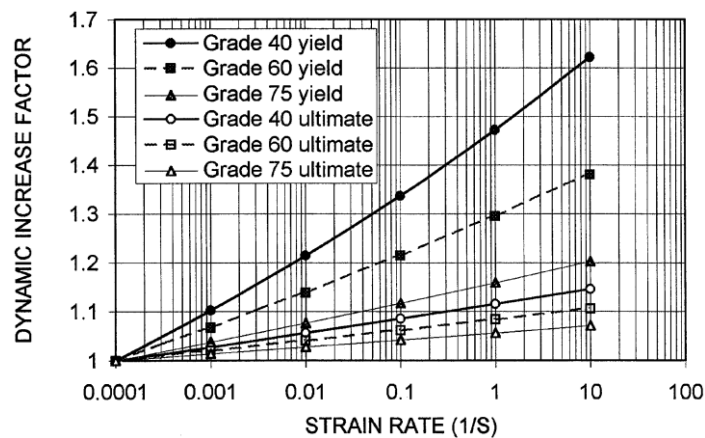


Figure 5. DIF for yield and ultimate stress of ASTM A615 steel reinforcing bars [15]

2.4 Determination of moment capacity

Determination of the DIFs based on the strain rate profile allows the force in each layer of the section to be calculated. For concrete this is given by eqn (10):

$$F_C = t_L b f_C(\epsilon) DIF(\dot{\epsilon}) \quad (10)$$

where t_L is the thickness of the layers in the sectional analysis, b is the width of the layer and $f_C(\epsilon)$ is the concrete stress. The force in the steel is calculated from eqn (11):

$$F_S = n A_S f_S(\epsilon) DIF(\dot{\epsilon}) \quad (11)$$

where, n is the number of reinforcing bars in a particular layer, A_S is the cross sectional area of the steel bar and $f_S(\epsilon)$ is the stress in the steel. The stress in both the concrete and steel are based on the stress-strain relationships shown in Figure 6a and b respectively. It is assumed that the Young's modulus of the material remains constant as the rate of loading increases, therefore only the yield strain increases as the dynamic strength increases. Fu et al. [12] reported on research showing that the Young's modulus of concrete in compression may actually increase at higher loading rates but no definitive relationships have been deduced so this effect has not been included in the current model. It is also assumed that the confinement provided by the FRP transverse wraps allows the concrete to sustain a much higher strain than normal prior to failure (ϵ_f) of up to 1% [17], as indicated in Figure 6a.

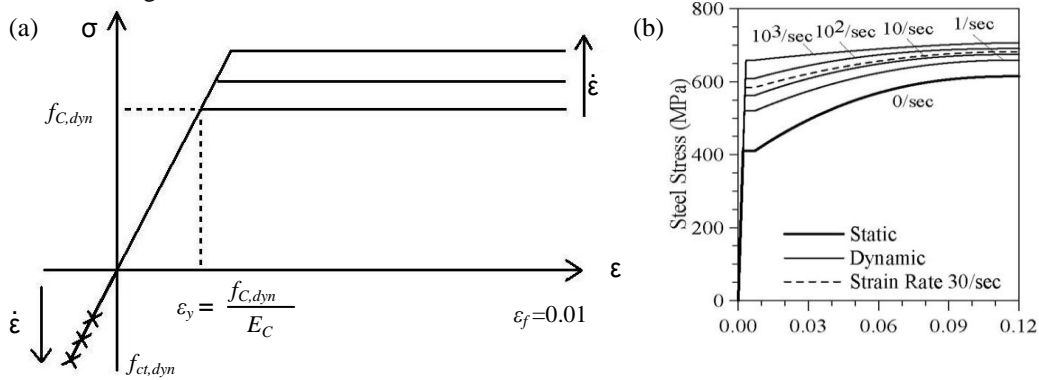


Figure 6. (a) Stress strain relationship with increasing strain rates used for concrete, (b) Stress strain relationship for steel with increasing strain rates [18]

The sum of the forces determined in each layer from eqns (10) and (11) must be in equilibrium with the applied forces. Achieving this usually requires the NA of the section to be determined iteratively, with the curvature kept constant as defined in eqn (9). Due to the added complexity of having to determine not only the strain and stress profiles but also strain rate profile, the iteration is best suited to numerical analysis. On attaining equilibrium of forces, moments are taken about a convenient location in the section to determine the member's moment capacity (M_P), from which the energy dissipated during the time step can be found from equation 2.

2.5 Energy dissipated and validation of initial assumptions

By assuming a hinge rotation (θ) at a particular time step, the moment capacity of the section and the energy dissipated can be determined as discussed. However, to ensure accuracy in the solution it is necessary to validate the assumption for the hinge rotation.

The assumed hinge rotation is validated by determining the mid-span displacement of the member from the assumed hinge rotation and comparing it with the displacement during the time step due to the change in kinetic energy of the member.

From the assumption of rigid body rotations the change in mid-span displacement during the n^{th} time step can firstly be calculated from simple trigonometry as:

$$\Delta\delta_\theta = \frac{L}{2} \tan(\theta_n) - \frac{L}{2} \tan(\theta_{n-1}) \quad (12)$$

where L is the height of the column. Determining the displacement from the motion of the member, as kinetic energy is dissipated, requires a slightly more involved analysis.

8 Plasticity Based Approach for Evaluating the Blast Response of RC Columns Retrofitted with FRP

It was discussed previously that the impulse from the blast wave causes the member to acquire kinetic energy, the acquisition of which will vary with time depending on the duration of the applied impulse. It is usually assumed that the pressure from the blast increases rapidly to the peak overpressure before decaying exponentially with time [9] (Figure 7a). From this relationship the time varying impulse can be found (Figure 7b), from which the kinetic energy of the member at the beginning of the time step can be determined. The initial kinetic energy (KE_{n-1}) at the beginning of the time step can then be rearranged in terms of the rotational velocity ($\dot{\theta}$) from equation 2 which can in turn be rearranged into the linear velocity of the mid-point (v_{n-1}) of the member from equation 13:

$$v_{n-1} = \frac{L}{2} \dot{\theta} \quad (13)$$

During the time step, kinetic energy is dissipated through plastic straining in the hinge regions. The kinetic energy at the end of each time step (KE_n) is then given by:

$$KE_n = KE_{n-1} - ED_n \quad (14)$$

where subscripts $n-1$ and n refer to the beginning and end of the time step and ED_n is the energy dissipated during the time step. The final kinetic energy at the end of the time step can then once again be rearranged in terms of the member's mid-height linear velocity (v_n). Assuming that suitably small time steps are chosen, the average velocity of the mid-point (v_{av}) during the time step can be approximated by eqn (15):

$$v_{av} = \frac{v_{n-1} + v_n}{2} \quad (15)$$

From this the change in displacement during the time step can be calculated:

$$\Delta\delta_v = v_{av}\Delta t \quad (16)$$

It is important at this stage to recognise that the initial assumption regarding the formation of a three hinge mechanism allows the above prediction of the displacement during the time step using rigid body dynamics.

If the correct value for the hinge rotation was assumed then the change in displacement determined from eqn (12) will be equal to that determined from eqn (16). If they are not equal then the initial assumption for the hinge rotation must be re-iterated. Through using this method for validating the assumed hinge rotation, the accuracy of the strain rate profile which has been used in the analysis can be confirmed, a key feature of the proposed model.

The process outlined above is subsequently repeated for additional time steps. At the beginning of a given time step the kinetic energy is taken as the final kinetic energy from the previous step combined with any additional kinetic energy from the blast impulse that is acquired by the member. The peak displacement of the member is finally determined when the kinetic energy of the member reaches zero by summing the displacements from each time step. The time for the member to reach its peak displacement can also be determined by summing the time steps.

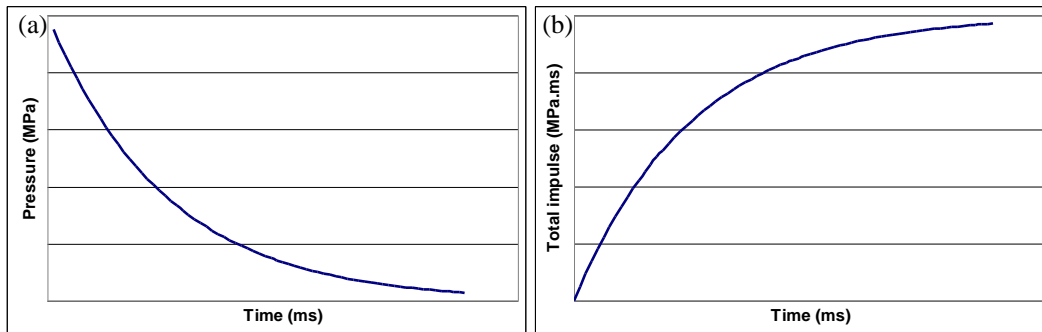


Figure 7: Typical force-time (a) and total impulse-time (b) relationships for blast loading

3. COMPARISON OF RESULTS

The results for the peak displacement predicted by the proposed model are compared against an elastic-perfectly plastic SDOF model [9] and experimental data [8, 19] in Figure 8.

The specimens tested in [8] and [19] were fixed at the supports and had cross-sectional dimensions of 356×356 mm and a clear height of 3227 mm with a concrete cylinder strength of 45 N/mm², 8 #8 ASTM A615 grade 60 longitudinal steel bars and CFRP transverse wraps which had a tensile modulus and rupture strength of 89 kN/mm² and 1544 N/mm² respectively. The general cross section layout is shown in Figure 2a. Test 6 [8] employed two layers of CFRP and Test 10 [19] used six layers. In both cases, the CFRP wrap was sufficient to prevent shear failure, leading to the formation of plastic hinges, as the model assumes. When comparing the results in [8] and [19] in the current analysis, a slight modification to the impulse is required based on the different assumed deflected shape used in these papers to convert the simulated blast test data to pressure-impulse relations.

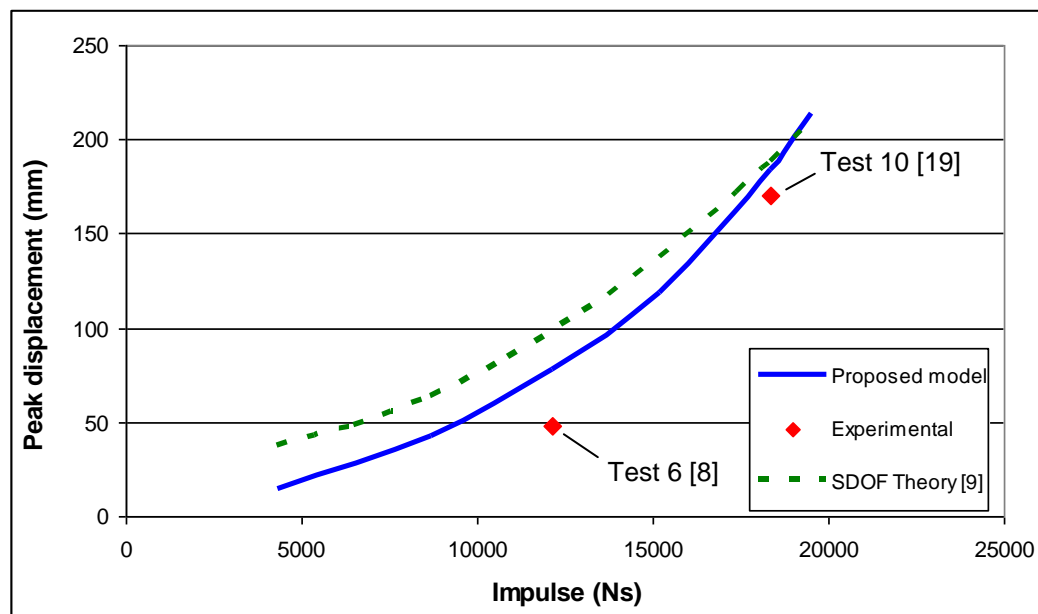


Figure 8. Graph of peak displacement predictions using the proposed plasticity model an elastic-perfectly plastic SDOF model [9] and experimental data

From Figure 8 it can be seen that the proposed model provides a conservative prediction for the peak displacement of the test results, however the proposed model shows an improvement over the equivalent SDOF method. The percentage error of the prediction of the higher energy test (Test 10) is approximately 8% whereas the prediction for the medium energy test (Test 6) is less accurate (around 60% greater than the measured result). It can also be seen that the trend from the proposed plasticity model better replicates the experimental data, although it is clearly apparent that more data is required.

It was expected that the proposed model would over-predict the response due to the assumption that all energy delivered from the blast event is dissipated as strain energy. It is therefore clear that further work is required to quantify other energy dissipation modes such as micro-crack growth and losses through heat and sound, amongst others and research is currently continuing in this area. The accuracy in predicting the lower impulse blast (Test 6) with the proposed plasticity model might be expected to be lower due to the lower relative magnitude of the plastic strains.

4 PARAMETRIC STUDY

In order to assess the efficacy of the proposed model a parametric study was conducted to validate some of the key assumptions. The predictions of the peak displacements of the tests carried out in [8] and [19] using the proposed plasticity model was based on some assumed parameters including:

1. The length of the plastic hinge, taken as $0.75h$
2. Characteristic values for the strength of the steel

Firstly the effect of the assumed plastic hinge length was investigated, the results of which are shown in Figure 9a. In the current formulation of the proposed model the plastic hinge length is required for determining the curvature in the section (eqn 9), from which the moment capacity and energy dissipation are determined. For the proposed model, a constant value for the hinge length of $0.75h$ was used, which was based upon that proposed by Wu et al. [11]. Figure 9a shows that a variation in the plastic hinge length between $0.65h$ and $0.85h$ ($\pm 13.3\%$ from $0.75h$) results in a maximum variation of the predicted peak displacement of test 10 [19] of just 1.9% . This suggests that the assumed length of the plastic hinge of $0.75h$ is acceptable. It should also be mentioned that an alternative method for determining the moment-rotation relationship, which does not require the plastic hinge length, is available [20]. However, this method is not suitable for the current model due to the lack of data on key parameters, in particular the shear friction material properties and reinforcement bond characteristics at high loading rates.

It is common in design that characteristic values are used for the strength of the materials, which leads to a conservative and safe design. However, in the case of the assessment of existing structures it becomes important to use representative material strengths in order to accurately predict the response. The predictions of the test results from [8] and [19] shown in Figure 8 used representative mean concrete strengths taken from actual cylinder tests, however, the steel strengths were taken as the characteristic value for ASTM A615 Grade 60 bars. Malvar [15] discussed a number of studies on these bars and showed that the average yield strength was approximately 15% greater than the characteristic strength (475 N/mm^2 compared with the characteristic value of 414 N/mm^2). Figure 9b shows how the predicted displacement of test 10 [19] (dotted line), changes when a steel with a yield strength of 475 N/mm^2 is used in both the proposed plasticity model and the equivalent SDOF method [9]. It can be seen that the accuracy of the proposed plasticity model increases by approximately 5% when more representative steel values are employed. It can also be seen that the accuracy of the equivalent SDOF method improved if more representative strength values were used, from a 10% error to just 3% .

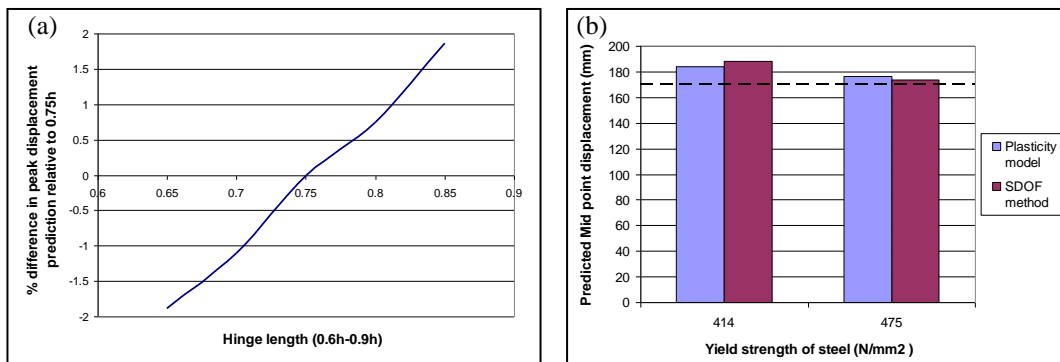


Figure 9. Parametric study on: (a) effect of plastic hinge length and (b) effect of steel yield strength on the proposed model and a SDOF model [9], compared with Test 10 [19]

Finally, a comparison was made between the upper bound prediction using the proposed plasticity model and a variety of SDOF predictions using different resistance functions. A significant advantage of the proposed plasticity model is the avoidance of having to arbitrarily select a resistance function. With the SDOF method one of three resistance functions can be selected [4]; elastic (e), elastic-perfectly plastic (e/pp) (which is an idealisation of the materials real behaviour) and elastic-plastic (e/p), which includes strain hardening and compression membrane effects. Shown in Figure 10 is the predictions for the peak displacement of test 10 [19] using the elastic-plastic, elastic-perfectly plastic, and the elastic-plastic function presented by Cormie [9] which is based on British Standards methods of analysis, compared with the proposed plasticity model. It can be seen that some variation exists in the predicted peak displacement for test 10 when different resistance functions are used in the equivalent SDOF method. The difference between the predictions using the elastic-plastic and elastic-perfectly plastic resistance functions is around 23% . It can be seen that the idealised elastic-perfectly plastic (e/pp) SDOF

prediction [4] is the most accurate, despite not being the most technically rigorous model of behaviour, which underlines one of the concerns over the SDOF method. The proposed plasticity model presented in the current paper is shown to be comparable to the SDOF predictions.

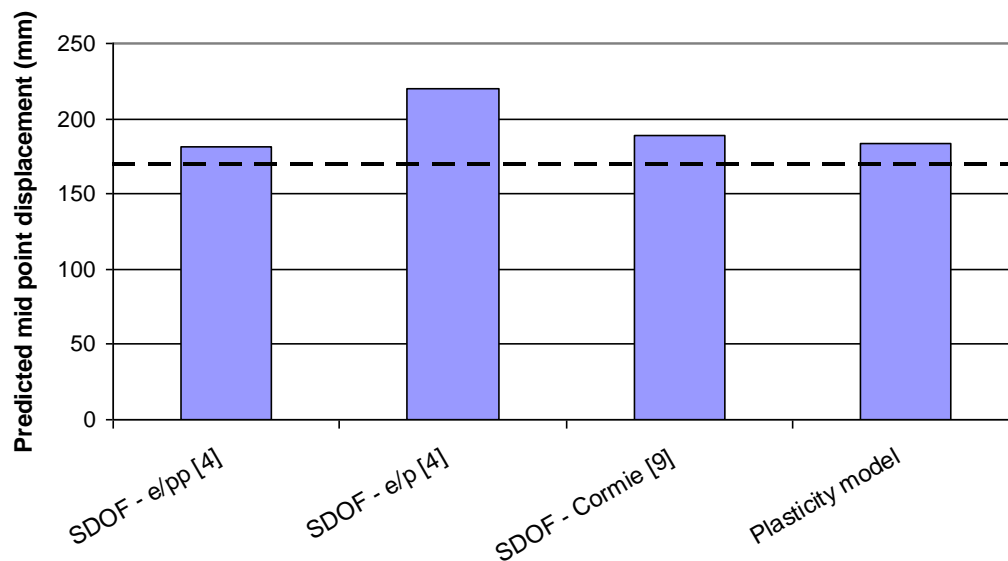


Figure 10: Comparison of predicted peak displacement of test 10 [19] through the use of different SDOF resistance functions and the proposed plasticity model

5. DISCUSSION

The results in Figure 8 demonstrates the potential of the proposed model to predict the response of RC columns subject to high energy blast loads and highlights the importance of accurate inclusion of the strain rate effects. The model appears less accurate at lower energies where plastic strains are less significant than in higher energy tests where deformations will be larger. Jones [21] showed that a plasticity model for impact can be accurate to within 10% when the ratio of the total energy to the elastic strain energy is greater than 10 and it is likely that a similar relationship exists for blast situations. Further to this it is likely that FRP retrofits would only be employed in situations where the risk of collapse was high. In these situations the member would be expected to sustain significant plastic deformations. Under these conditions it is stated in the UFC guidelines [10] that the elastic and elasto-plastic ranges of response can be ignored and only the plastic behaviour need be considered.

The main assumptions of the proposed model are that plastic hinges have formed simultaneously from the outset of the deformation, that all of the supplied energy is converted to plastic strain energy in the hinges and that shear failure cannot occur. As the model is primarily intended to analyse structures with large deformations, neglecting the elastic and elasto-plastic ranges of response is likely to be acceptable. The assumption regarding all the energy being dissipated in the plastic hinges is likely to be the biggest source of error in the model with alternative energy dissipation modes such as the creation of new surface area in micro-crack growth, heat and sound also contributing to the behaviour. The assumption that shear failure has been prevented does not address the design requirements for the FRP transverse wraps although this is not the premise of the current paper and is the subject of further work.

The primary advantage of the proposed plasticity model over the equivalent SDOF method is the ease and accuracy in calculating strain rates in the materials and the ability to directly apply these in the analysis, throughout the response period of the structure. It was alluded to by El-Dakhkhni *et al.* [6] that no simple method exists for accurately calculating the strain rates. This led Cormie *et al.* [9] to suggest using constant values that are known to be conservative. The incremental approach of the current model has overcome this problem and allows accurate strain rates to be determined simply. Additionally, the incremental approach allows full inclusion of the time varying nature of the applied loading and improved representation of material characteristics such as strain hardening and concrete in tension. Other benefits of the model include the avoidance

of arbitrarily selecting a resistance function and the prediction of the peak displacement being a known upper bound.

6. CONCLUSION

An alternative to the SDOF method is presented, based on plasticity theory, to predict the peak displacement of a FRP retrofitted RC column deforming flexurally. The model provides a convenient and simple method for accurately assessing the changes in strain rates over time and variations in strain rate across the section, which have an important effect on material strength. The proposed model also has the advantage of not requiring the selection of a resistance function as is the case with the equivalent SDOF method.

The model is primarily intended to assess RC columns retrofitted with FRP under high energy blasts which typically result in plastic hinge formation rather than shear failure, and is shown to give good predictions for the peak displacement in this case, although it appears that some energy is dissipated by other means, not accounted for. Through the use of a direct energy method, without using transformation factors, the method can be easily extended in the future to include energy dissipative modes such as spalling and fragmentation of the concrete in un-retrofitted members. This will lead to a more accurate representation of the true behaviour of a member subjected to a blast load than is currently possible with alternative analytical models. Characterising the energy dissipated by these other modes of damage is the subject of further work.

ACKNOWLEDGEMENTS

Sincere thanks are extended to Dr Tona Rodriguez-Nikl for his assistance in providing experimental data, Professor Pedro Silva for useful discussions and to the University of Bath for providing funding for this work.

REFERENCES

- [1] Malvar LJ, Crawford JE, Morrill KB, Use of composites to resist blast, *Journal of Composites for Construction*, 2007, 11, 601-610
- [2] Buchan PA, Chen JF, Blast resistance of frp composites and polymer strengthened concrete and masonry structures - a state-of-the-art review, *Composites Part B-Engineering*, 2007, 38, 509-522
- [3] Biggs JM, *Introduction to structural dynamics*, New York: McGraw-Hill, 1964.
- [4] Rodriguez-Nikl T, Kobayashi T, Oesterle MG, Lan S, Morrill KB, Hegemier GA, Seible F, Carbon fiber composite jackets to protect reinforced concrete columns against blast damage, *Structures Congress 2009: Don't Mess with Structural Engineers - Expanding Our Role*, 2009,
- [5] Razaqpur G, Mekky W, Foo S, Fundamental concepts in blast resistance evaluation of structures, *Canadian Journal of Civil Engineering*, 2009, 36, 1292-1304
- [6] El-Dakhakhni WW, Rezaei SHC, Mekky WF, Razaqpur AG, Response sensitivity of blast-loaded reinforced concrete structures to the number of degrees of freedom, *Canadian Journal of Civil Engineering*, 2009, 36, 1305-1320
- [7] Crawford J, Magallanes JM, The effects of modeling choices on the response of structural components to blast effects, *First International Conference of Protective Structures*, 2010,
- [8] Rodriguez-Nikl T, Experimental simulations of explosive loading on structural components: Reinforced concrete columns with advanced composite jackets, 2006, PhD,
- [9] Cormie D, Mays GC, Smith PD, *Blast effects on buildings*, London: Thomas Telford Limited, 2009.
- [10] UFC-3-340-02, Structures to resist the effect of accidental explosions us department of the army, navy and air force technical manual., 2008,
- [11] Wu CQ, Oehlers DJ, Day I, Layered blast capacity analysis of frp retrofitted rc member, *Advances in Structural Engineering*, 2009, 12, 435-449

- [12] Fu HC, Erki MA, Seckin M, Review of effects of loading rate on concrete in compression, *J. Struct. Eng.-ASCE*, 1991, 117, 3645-3659
- [13] Soroushian P, Obaseki K, Strain rate-dependent interaction diagrams for reinforced concrete sections, *ACI Journal*, 1986, 83, 9
- [14] Malvar LJ, Crawford JE, Dynamic increase factors for concrete, *Twenty-Eighth DDESB Seminar*, 1998,
- [15] Malvar LJ, Review of static and dynamic properties of steel reinforcing bars, *Acı Materials Journal*, 1998, 95, 609-616
- [16] Bischoff PH, Perry SH, Compressive behavior of concrete at high-strain rates, *Mater. Struct.*, 1991, 24, 425-450
- [17] Concrete Society., Design guidance for strengthening concrete structures using fibre composite materials, *Technical Report No. 55*, 2004,
- [18] Silva PF, Lu BG, Blast resistance capacity of reinforced concrete slabs, *J. Struct. Eng.-ASCE*, 2009, 135, 708-716
- [19] Hegemier G, Seible F, Karbhari V, Lee C, Rodriguez-Nikl T, Oesterle M, Hutchinson T, Morrill K, Crawford J, The use of fiber reinforced polymers to mitigate natural and man-made hazards, *FRPRCS-8*, 2007,
- [20] Haskett M, Oehlers DJ, Ali MSM, Wu CQ, Rigid body moment-rotation mechanism for reinforced concrete beam hinges, *Engineering Structures*, 2009, 31, 1032-1041
- [21] Jones N, *Structural impact*, Cambridge: Cambridge University Press, 1989.